PC5228 Report

Peter Sidajaya
A0170766X

October 2021

In this assignment, we run a Mach-Zehnder Interferometer on a Quantum Computer using IBM's IBMQ platform here.

1 Introduction

Originating as an optical interferometer used to measure the relative phase shift between mediums, the Mach-Zehnder Interferometer [1] is a device often used to introduce students to the concept of two-level quantum systems (qubit). It starts with a single collimated source directed to a beamsplitter. The beamsplitter splits the beam into two beams ('upper' and 'lower'). A phase shifter (or a test medium) is then placed on one of the beams to cause an optical path difference. The two beams are then reflected each by a a mirror to another beamsplitter. Detectors are then put at the output arms of the beamsplitter to measure the intensity of light on each output port of the beamsplitter.

Using the electromagnetic wave description of light, it is possible to predict the relationship of the intensity of light with the phase of the phase shifter. What is surprising, however, is that this relationship still holds when instead of a coherent beam of light, single photons are used as the source (or a quantum particle, such as an electron). The intensity then translates to the probability of detection for a single photon at each output. This phenomenon exemplifies the wave-particle duality that is so peculiar to quantum theory.

In the language of quantum computer, we can describe this experiment by a simple quantum circuit consisting of a Hadamard gate, a phase gate, another Hadamard gate, and then a measurement. Figure 1 shows the circuit diagram for the interferometer.

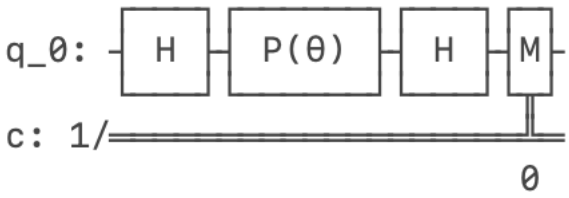

Figure 1: Circuit diagram of Mach-Zehnder Interferometer

2 Theory behind the Interferometer

In the qubit description of the interferometer, the action of the interferometer (before the final measurement) is equivalent to the evolution

$$|\psi\rangle \longrightarrow HP(\theta)H\,|\psi\rangle \tag{1}$$

[1] referred as 'the interferometer' from now on

on an input qubit $|\psi\rangle$. Let $|0\rangle$ denotes the 'upper' arm and $|1\rangle$ the 'lower' arm.

$$|0\rangle = \begin{pmatrix} 1 \\ 0 \end{pmatrix}, \qquad |1\rangle = \begin{pmatrix} 0 \\ 1 \end{pmatrix} \tag{2}$$

Without loss of generality, we can say that the light comes in from the upper arm. We then apply a Hadamard gate, which describes the action of the beamsplitter to the light. The Hadamard gate is given by

$$H = \frac{1}{\sqrt{2}} \begin{pmatrix} 1 & 1 \\ 1 & -1 \end{pmatrix}. \tag{3}$$

The minus here refers to the phase shift that must be incurred by the beamsplitter [2]. The phase gate, which are described by

$$P(\theta) = \begin{pmatrix} 1 & 0 \\ 0 & e^{i\theta} \end{pmatrix}. \tag{4}$$

describes the action of applying the phase shifter on the lower arm. The final Hadamard gate describes the second beamsplitter. The final state is then given by

$$HP(\theta)H\,|0\rangle = e^{i\frac{\theta}{2}} \begin{pmatrix} \cos\left(\frac{\theta}{2}\right) \\ -\sin\left(\frac{\theta}{2}\right) \end{pmatrix}. \tag{5}$$

The probability of detection on the upper arm of the detector is then given by

$$P(|0\rangle \mid \theta) = \cos^2\left(\frac{\theta}{2}\right). \tag{6}$$

This interference pattern is what we are looking for in this experiment. In the code and in further discussion, we will call this the '0 count' due to the fact that we denote the upper arm by $|0\rangle$.

Furthermore, interferometric visibility is defined as

$$\nu = \frac{A}{\bar{I}}. \tag{7}$$

where A is the envelope and $\bar{I}$ is the average intensity. In terms of intensities, it can be rewritten as

$$\nu = \frac{I_{max} - I_{min}}{I_{max} + I_{min}}. \tag{8}$$

For a quantum treatment, we can swap the intensity with probabilities. From equation 6, we can see that, for an ideal interferometer, the maximum probability is 1, given by $\theta = 0$, and the minimum is 0, given by $\theta = 2\pi$. Thus, for an ideal interferometer, $\nu = 1$. This quantity gives a measure of how good is the experimental pattern that we see.

3 Interferometer Results

The result of the interferometer is laid out in Figure 2. Error bars of one standard deviation are plotted in the code but they are too small to be seen. We can see that the general shape of the interference are in agreement with our prediction (equation (6)) in the previous section.

In order to find the visibility of the interference, we first fit a curve to the data. The equation we fit is

$$f(\theta) = \frac{1 + \nu\cos(\theta + d)}{2}$$

where ν is the visibility that we want. We allow a bias error in the phase by adding d to the function. It can be checked that by substituting the maximum and minimum points of $f(\theta)$, equation 8 is fulfilled.

[2] there are different descriptions of the phase shifts of a beamsplitter, depending on the geometry. However, they all give the same resulting interference here.

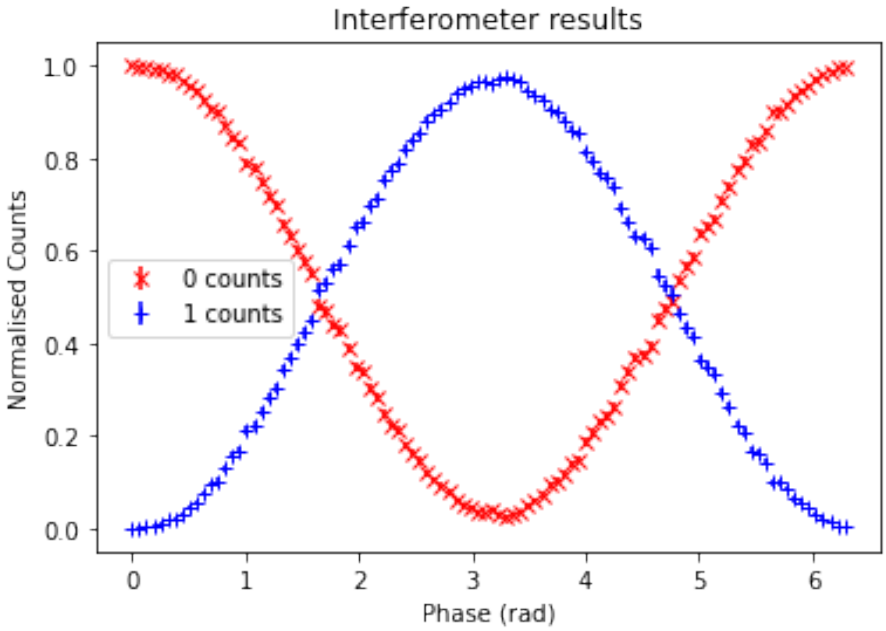

Figure 2: The result of the interferometer circuit run on IBMQ Belem. Error bars of one standard deviation are plotted but are too small to be seen.

We fit the data using non-linear least squares. From our fit, we find the value of the visibility to be 0.964 ± 0.005.

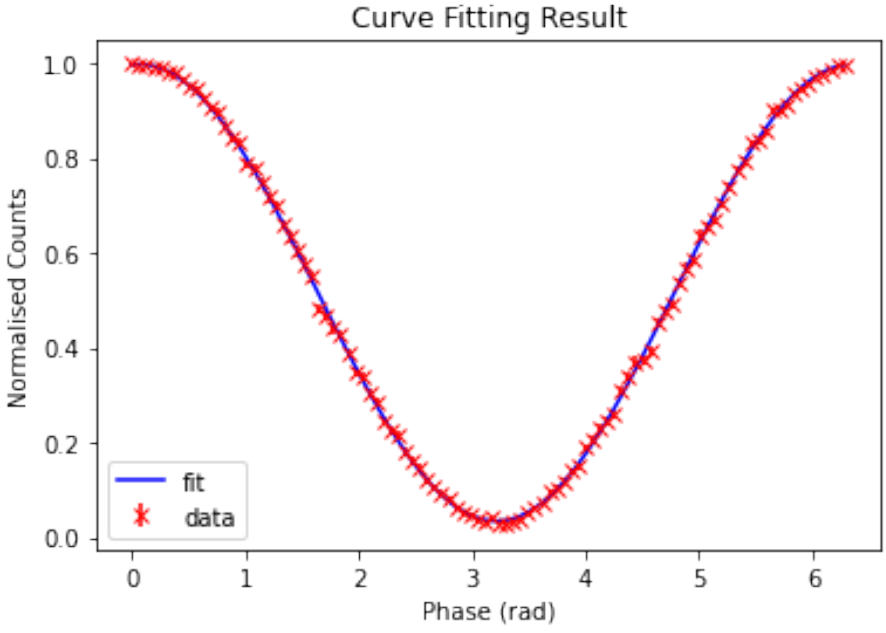

Figure 3: The result of the fitting. Error bars of one standard deviation are plotted but are too small to be seen. We ignore them for the fitting.

This value is very high, as it almost reaches one. This shows that for this task of showing the interference pattern, the noise in IBMQ Belem does not pose a serious problem. While current quantum computers are notorious for its noise, and IBMQ Belem is no exception, Mach-Zehnder interferometry is a relatively simple task with a small circuit. Thus, we could still obtain a good result in spite of its noises.

4 Entanglement and Decoherence

This part is inspired by Lecture 14. Let us consider the following circuit. Before the application of a phase gate, we apply a controlled RX gate to an ancilla qubit. The rest of the interferometer proceeds as usual.

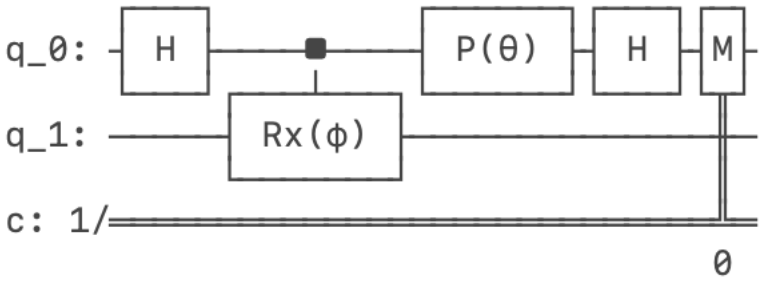

Figure 4: Caption

The RX gate rotates the Bloch Sphere by the X-axis, and it is defined as

$$RX(\phi) = \exp\left(-i\frac{\phi}{2}X\right) = \begin{pmatrix} \cos\left(\frac{\phi}{2}\right) & -i\sin\left(\frac{\phi}{2}\right) \\ -i\sin\left(\frac{\phi}{2}\right) & \cos\left(\frac{\phi}{2}\right) \end{pmatrix}. \tag{9}$$

The action of the controlled RX gate will entangle the system with the ancilla, and the degree of the entanglement will depend on the ϕ parameter of the RX gate. The ϕ parameter describes the amount of rotation done on the ancilla, and $\phi = 0$ is equivalent to no rotation, while $\phi = \pi$ is rotates the sphere by 180°.

From Lecture 14, we can see that the visibility will decrease as the action of the controlled unitary becomes more distinguishable. In our case, this means that as ϕ increases, visibility will decrease. From the notes in Lecture 14, the visibility is given by

$$\nu = |\langle\psi| RX(\phi) |\psi\rangle| = \cos\left(\frac{\phi}{2}\right). \tag{10}$$

This expression can also be found by finding the difference in the maximum and minimum probabilities of the interference pattern in the current circuit.

An intuition can be gained from the observation that when $\phi = \pi$, the controlled RX gate transforms the system and the ancilla into a Bell state. Since the partial state of a Bell state is just the random noise state $\frac{\mathbb{I}}{2}$, when we do a measurement on random noise, we would get zero interference visibility.

Now, we run this experiment on IBMQ Belem.

From Figure 5, we can see that the amplitude of the interference pattern decreases as we increase the rotation angle ϕ of the RX gate. At its maximum (brightest line), the interference almost completely dies out.

Using the same method as in the previous section, we can see how the visibility is affected by the rotation angle. The result is given in Figure 6. It can also be seen that our experimental result roughly agrees with the theoretical prediction made in equation 10. It does not match it perfectly, however. In the case of $\phi = \pi$, it should theoretically be complete noise independent of the phase, but we can still see a pattern. While in the case of $\phi = 0.35$, there is a dramatic decrease in visibility, which is more than the theoretical treatment predicts. Moreover, it seems that the minimum point shifts to the right as ϕ gets larger, which is unexpected. The source of these errors could lie in the errors in the devices and the noises of the computer, but it is outside the scope of the report to analyse them in detail.

The result of this circuit can give some insights into how noise creeps in in a quantum computer. As we have seen, the degree of the interaction between the system with the ancilla disrupts the quality of the interference. In a quantum experiment, we can imagine the the environment surrounding the system as the ancilla. The interaction between the system and the environment plays the role of the RX gate

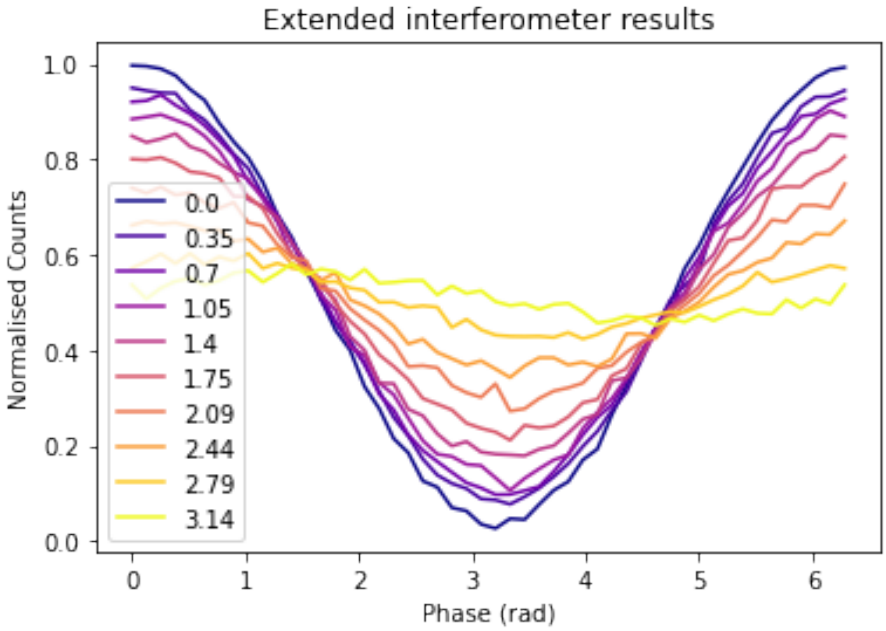

Figure 5: The result of the extended interferometer. The different colours label the different rotations of the RX gate.

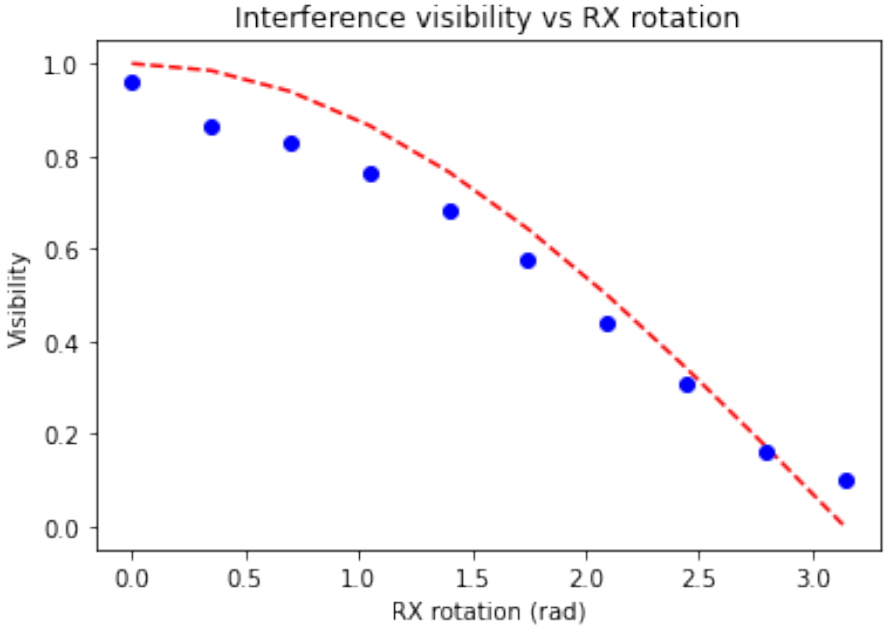

Figure 6: The visibilities of the result. The dotted line is the theoretical prediction from equation (10)

which entangles them to each other. This entanglement, in turn, leads to decoherence in the system. Practically, this means a lowering of the interferometric visibility when we try to measure the system. This leads to lower fidelity when trying to do other computations.

5 Conclusion

In this report, we have run a Mach-Zehnder Interferometer on a quantum computer by IBMQ. We have analysed the quality of the interference with the notion of visibility. Using nonlinear fitting, we found our

interference pattern to have a visibility of 0.964 ± 0.005, which is good. We have also run an extended Mach-Zehnder Interferometer where we entangle the system with an ancilla to various degrees. This leads to a decrease of visibility, which we have shown.

6 Code

Relevant codes and results are inside my GitHub repository https://github.com/PeterSidajaya/PC5228-analysis.

- `PC5228_data_generation.ipynb` generates the data for section 3. The data is stored in the `data` folder.
- `PC5228_data_generation_extended.ipynb` generates the data for section 4. The data is stored in the `data_extended` folder.
- `PC5228_analysis.ipynb` generates the figures and analysis for 3.
- `PC5228_analysis_extended.ipynb` generates the figures and analysis for 4.

A Uncertainty of Experimental Data Points

In this report, we have previously mentioned that the error bars are to small to be seen and to affect the subsequent fitting. In this appendix, we will demonstrate how we calculated the uncertainty. The resources we used for this part can be found here and here.

Let the measurement probability be denoted by p. Since it is a two-outcome process, it is a Bernoulli process. The experimental data points $\hat{p} = \sum_i \frac{x_i}{n}$ are the estimators of p. Since the process are repeated numerous times and are independent, we can use the Central Limit Theorem. Under the CLT,

$$\hat{p} = \sum_i \frac{x_i}{n} \sim N\left(p, \frac{\hat{p}(1-\hat{p})}{n}\right).$$

Thus, $\sigma = \sqrt{\frac{\hat{p}(1-\hat{p})}{n}}$. Since the circuit were run with 2048 shots, the maximum value of the standard deviation (obtained when $\hat{p} = 0.5$) is only 0.011, too small to be seen and can safely be neglected for the fitting process.